

Published in final edited form as:

Free Radic Biol Med. 2010 December 1; 49(11): 1666–1673. doi:10.1016/j.freeradbiomed.2010.08.026.

AN OXIDATIVE ENVIRONMENT PROMOTES GROWTH OF *MYCOBACTERIUM ABSCESSUS*

Rebecca E. Oberley-Deegan¹, Brittany W. Rebits¹, Michael R. Weaver¹, Angela K. Tollefson¹, Xiyuan Bai^{1,2}, Mischa McGibney^{1,2}, Alida R. Ovrutsky^{1,2}, Edward D. Chan^{1,2}, and James D. Crapo¹

¹Department of Medicine, National Jewish Health, Denver CO, 80206

²Department of Medicine, Denver VA Medical Center, Denver CO, 80220

Abstract

Mycobacterium abscessus (*M. abscessus*) infections, particularly those causing chronic lung diseases, are becoming more prevalent worldwide. *M. abscessus* infections are difficult to treat due to antibiotic resistance. Thus, new treatment options are urgently needed. *M. abscessus* are intracellular pathogens that primarily infect macrophages and fibroblasts. Because this bacterium has only recently been identified as a separate species, very little is known about *M. abscessus*-host interactions and how *M. abscessus* growth is regulated. Oxidative stress has long been shown to inhibit growth of bacterial organisms. However, some intracellular bacteria, such as *Mycobacterium tuberculosis*, grow well in oxidizing environments. In the present study, we show that *M. abscessus* infection causes the host cell environment to become more oxidizing. Furthermore, we show that a more oxidizing environment leads to enhanced growth of *M. abscessus* inside macrophages. In the presence of the antioxidants, MnTE-2-PyP (chemical name: Manganese (II) Meso-Tetrakis-(N-Methylpyridinium-2-yl) porphyrin) or N-acetyl-L-cysteine (NAC), *M. abscessus* growth is inhibited. These results lead us to postulate that antioxidants may aid in the treatment for *M. abscessus* infections.

Keywords

Mycobacterium abscessus; oxidation; antioxidants; MnTE-2-PyP; N-acetyl-L-cysteine; THP-1; alveolar macrophages; smoking

Introduction

Mycobacterium abscessus (*M. abscessus*) are rapidly growing nontuberculous mycobacteria (NTM). *M. abscessus* are intercellular pathogens that primarily infect and reside in macrophages and fibroblasts of the lungs and skin [1]. The prevalence of rapidly growing NTM infections, such as *M. abscessus*, is increasing in the United States and throughout the world [1–4]. For example, a recent study reported a mean annual increase of 8.4% for NTM infections

© 2010 Elsevier Inc. All rights reserved.

Address correspondence: Rebecca E. Oberley-Deegan, Ph.D., Department of Medicine, National Jewish Health, Denver, CO, 80206 USA, FAX: 303-270-2249, Telephone: 303-398-1749, oberleyr@njc.org.

Publisher's Disclaimer: This is a PDF file of an unedited manuscript that has been accepted for publication. As a service to our customers we are providing this early version of the manuscript. The manuscript will undergo copyediting, typesetting, and review of the resulting proof before it is published in its final citable form. Please note that during the production process errors may be discovered which could affect the content, and all legal disclaimers that apply to the journal pertain.

and a 9.6% increase in rapidly growing NTM infections from years 1997 to 2003 [5]. There are few known risk factors for developing NTM lung infections although there is some evidence of familial clustering of NTM infections [6].

M. abscessus lung infections are particularly difficult to treat. Currently, there are only two treatment options available for patients afflicted with *M. abscessus* infections: antibiotic regimen with or without surgical resection of the affected lung tissue. Unfortunately, *M. abscessus* is resistant to most antibiotics and treatment with effective antibiotics only leads to about a 50% long term cure rate [7]. Ballarino *et al.* showed that patients with *M. abscessus* lung infections have a 4.2 fold increased likelihood of having more extensive lung disease than lung disease caused by other NTM [8]. Novel treatment options for *M. abscessus* infections are urgently needed.

Relatively little is known about *M. abscessus* infections, in part because *M. abscessus* has only been identified as a separate species since 1992 [7]. Understanding the dynamics between *M. abscessus* bacteria and the host immune cells still need further characterization. Our previous work showed that an antioxidant mimetic, MnTE-2-PyP, inhibits the intracellular growth of *M. abscessus* [9]. This indicates that the cell redox environment may play a role in *M. abscessus* bacterial growth intracellularly.

While it is generally true that an oxidative environment helps to kill bacterial organisms, select intracellular pathogens are able to withstand hostile oxidative environments inside the cell. Indeed, another mycobacterium, *Mycobacterium tuberculosis*, grows better in macrophages at high oxygen concentrations [10]. Tuberculous lesions are often present in areas with high tissue PO₂, such as lung apices, indicating that *M. tuberculosis* preferentially grows in oxidative environments [10]. In addition, oxidative stress triggered by infection causes damage to host tissues. Recent studies have shown that a reduction in oxidative stress protects host tissues from damage by reducing inflammation associated with infection. Mita *et al.* showed that metallothionein, a reactive oxygen species (ROS) scavenger, protected mice against *Helicobacter pylori*-induced gastric lesions by reducing inflammatory cell activity [11]. Similarly, influenza-infected mice treated with the antioxidant mimetic, MnTE-2-PyP (chemical name: Manganese (II) Meso-Tetrakis-(N-Methylpyridinium-2-yl) porphyrin), had reduced immunopathology and increased macrophage numbers in their airways [12]. Together these studies set a precedence suggesting that oxidative stress induced by infection may be more detrimental to the host than facilitative in killing the bacteria.

In the present study, we investigated the role that oxidative stress plays in *M. abscessus* infection in an *in vitro* model of infection using a human monocytic cell line. We hypothesized that decreasing the oxidizing environment, to which *M. abscessus* have become adapted, will reduce intracellular bacterial viability. We found that a *M. abscessus* infected cell had a more oxidizing environment as compared to an uninfected cell. In addition, we determined that *M. abscessus* grew better in a more oxidizing environment and that in the presence of antioxidants intracellular *M. abscessus* viability was reduced.

Materials and Methods

THP-1 Cell Growth

THP-1 cells, a human monocyte-derived cell line, were obtained from the American Type Culture Collection (ATCC, Manassas, VA). The cells were grown as previously described [9].

M. abscessus Preparation

M. abscessus was obtained from ATCC and prepared as previously described [9].

Culture, Infection and Harvesting of THP-1 Cells

THP-1 cells (1×10^6 cells) were treated with RPMI media with 10% fetal bovine serum containing PMA (7.5 ng/mL) for 24 hours. Cell medium was replaced with fresh 10% FBS RPMI medium with or without MnTE-2-PyP (30 μ M). After 1 hour incubation, the cells were infected with 1×10^7 bacteria/well (MOI = 10) for 1 hour. The infectious medium was removed and replaced with fresh 10% FBS RPMI with or without MnTE-2-PyP. For the 0 hour time point, the medium was removed and replaced with 1 mL of cold 1X PBS. Adherent cells were then scraped from the plate and centrifuged at $300 \times g$ for 5 minutes. The supernatants were removed and the pellets were resuspended in 100 μ l of lysis buffer (50 mM Tris-HCL, pH 8.0, 120 mM NaCl, 1% NP40, 5 mM EDTA and protease inhibitor cocktail tablet (Roche Diagnostics, Mannheim, Germany) for western blot analysis and activity assays for MnSOD, Cu/ZnSOD and catalase. For glutathione peroxidase (GPx) activity assays, a different lysis buffer was used (50 mM Tris-HCl pH 7.5, 5 mM EDTA, and 1 mM DTT). The cell pellets collected for the reduced glutathione (GSH) assay were frozen at -80°C immediately after the removal of the supernatant and were not resuspended in lysis buffer.

MnSOD and Cu/ZnSOD Real Time RT-PCR Analysis

THP-1 cells (1×10^6 cells) were treated with RPMI media containing PMA (7.5 ng/ml). After 24 hours, the cells were adhered to the plate and the medium on the cells was replaced with fresh 10% FBS RPMI. The cells were infected with 1×10^7 bacteria/well (MOI = 10) for 1 hour. For all wells, the infectious medium was removed and replaced with fresh 10% FBS RPMI. Cells were harvested at 0, 6, 24 and 48 hours post-infection and RNA was extracted from adherent cells using a RNeasy Mini Kit (Qiagen, Valencia, CA) according to manufacturer's instructions. The total RNA concentration for each sample was measured using a spectrophotometer at 260 nm. The quality of the RNA was determined by measuring the ratio of the absorbance read at 260 and 280 nm ($A_{260}:A_{280}$). One ng of each sample was loaded in triplicate onto 96-well real time fast plates (LightLabs Inc, Dallas, TX). The TaqMan RNA-to-CT 1-Step Kit (Applied Biosystems, ABI, Foster City, CA) was used according to manufacturer's instructions with ABI TaqMan primers for MnSOD, Cu/ZnSOD and 18S gene. The plate was run through the following thermocycle: 48°C for 15 minutes, 95°C for 10 minutes, (95°C for 15 seconds, 60°C for 1 minute) X 40 cycles. Relative MnSOD and Cu/ZnSOD mRNA levels were assessed by the comparative quantitation method and calculated difference in mRNA expression were determined according to the manufacturer User Bulletin 2 (10/2001, ABI).

Immunoblot Analysis

THP-1 cells were infected and lysed as described above and cells were harvested 0, 24, 48 and 72 hours post-infection. Total protein content for each sample was determined by using a bicinchoninic acid (BCA) kit (Peirce, Rockford, IL). The samples, 50 μ g, were loaded on a 12% Tris-HCl gel under denaturing conditions. After the gels were electrophoresed for 2 hours at 150 V, the separated proteins were transferred onto a nitrocellulose membrane for 1 hour at 100 V. The blots were blocked in 5% Blotto (dried milk diluted in PBS) for 1 hour, then incubated overnight at 4°C with 1:10,000 anti-MnSOD and 1:5,000 anti-Cu/ZnSOD antibodies that were diluted in 5% Blotto. The antibodies were a kind gift from Dr. Frederick Domann at the University of Iowa. Blots were washed in 0.1% Tween 20 in PBS (PBST) five times for 5 minutes per wash, then incubated with 1:50,000 of goat anti-rabbit conjugated to horseradish peroxidase diluted in PBST (Jackson Laboratories, West Grove, PA) for 1 hour at room temperature. The blots were washed again in PBST five times for 5 minutes per wash and then incubated for 1 minute with ECL substrate (Pierce). To ensure equal protein loading, blots were stripped and probed for β -actin. A primary mouse anti-human β -actin antibody (Sigma, St. Louis, MO) was used at 1:10,000 followed by a secondary donkey anti-mouse secondary

that was conjugated to horseradish peroxidase (1:50,000, Jackson Laboratories). The blots were exposed to film and densitometry was performed on the MnSOD and Cu/ZnSOD bands.

MnSOD and Cu/ZnSOD ELISA

THP-1 cells were infected and lysed as described above and cells were harvested 0, 24, 48 and 72 hours post-infection. Total protein content for each sample was determined by using a BCA kit (Pierce). Lysates were diluted 1:500 for Cu/ZnSOD ELISA (eBioscience, San Diego, CA) and 1:100 for the MnSOD ELISA (Northwest Life Science Specialties, Vancouver, WA). The samples were run according to the manufacturer's instructions and the data was normalized as a ratio of SOD protein to the total amount of protein per sample.

MnSOD and Cu/ZnSOD Activity Gel Assay

THP-1 cells were infected and lysed as described above. Cells were harvested at 0, 24, 48 and 72 hours post-infection. Total protein content for each sample was measured using a BCA kit (Pierce). In some cases 10% FBS RPMI, FBS, or *M. abscessus* were analyzed. Equal amounts of protein (100 μ g) were electrophoresed on a 12% Tris-HCl gel in non-denaturing running buffer (12.1 g Tris Base, 57.6 g glycine into 4 L ddH₂O). Gels were run for 2–3 hours at 150 V and were rinsed in ddH₂O for 5 minutes. Gels were then rocked in nitroblue tetrazolium (NBT) dye (40 mg NBT, 85 μ l TEMED, and 4 μ l of riboflavin stock (53 mg/mL of riboflavin) in 20 mL of ddH₂O) for 20 minutes while protected from light. The dye was removed and gels were washed 3 times for 5 minutes per wash in ddH₂O. The gel was exposed to bright fluorescent light until achromatic bands were clearly visible [13]. Gels were dried at 80 °C for 2 hours. Densitometry was then performed on the achromatic bands.

Catalase Activity Gel Assay

THP-1 cells were infected and lysed as previously described. Cells were harvested at 0, 24, 48 and 72 hours post-infection. Total protein content for each sample was determined using a BCA kit (Pierce). The proteins (50 μ g) were run on a 7.5% Tris-HCl gel in nondenaturing running buffer (12.1g Tris Base, 57.6 g glycine into 4 L ddH₂O) for 2–3 hours at 150 V. Gels were washed 3Xs in ddH₂O for 10 minutes per wash. Gels were incubated in 0.003% H₂O₂ for 10 minutes, and then quickly rinsed twice in ddH₂O. The gels were placed in dye (2% Ferric chloride and 2% Potassium ferricyanide) until achromatic bands formed, then the gel was removed and washed in ddH₂O 3Xs, 10 minutes per wash [13]. Gels were dried in gel dryer at 80 °C for 2 hours. Densitometry was performed on the achromatic bands.

Glutathione Peroxidase Activity Assay (GPx)

THP-1 cells were infected and lysed as described in previous sections and cells harvested 0, 24, 48 and 72 hours post-infection. Total protein content was determined for each sample using a BCA kit (Pierce). Total GPx activity for each sample was measured using the Cayman Chemical Glutathione Peroxidase Assay Kit (Cayman Chemical, Ann Arbor, MI). Results were obtained and analyzed according to manufacturer's instructions. The calculated GPx activity was normalized to the amount of protein present in each sample.

Glutathione Assays

THP-1 cells were infected and collected as described previously. Cells were collected at 0, 10, 30, 60, 120 and 240 minutes post-infection. Frozen cell pellets were thawed on ice and resuspended in 200 μ l cold PBS. In each sample, cells were sonicated for 5 seconds, and then centrifuged at 20,000 \times g for 5 minutes. The supernatant was collected and the total protein content for each sample was measured using a BCA kit (Pierce). All reagents for the GSH or GSSG assay were suspended in KPE buffer (16 mL of 100 mM KH₂PO₄, 84 mL of 100 mM K₂HPO₄, pH 7.5, 327 mg EDTA). GSH was measured against a known standard curve of GSH

and GSSG was measured against a known standard curve of GSSG. For the GSSG assay, the cell lysate was incubated with 0.6% sulfosaclicylic acid and 2-vinylpyridine for one hour followed by a 10 minute incubation of triethanolamine. The samples were spun at $20,000 \times g$ for 5 minutes. Samples for GSH and GSSG then had 100 μ l of 5,5' dithiobis-2-nitrobenzic acid/ glutathione reductase (DTNB/GR buffer: 2 mg DNTB/ 3 mL of KPE; 750 U glutathione reductase/ 3 mL of KPE) added to 20 μ l of sample or standard. To initiate the kinetic reaction, 50 μ l of β – NADPH solution (2 mg β – NADPH / 3 mL of KPE) was added to each well, and the plate was immediately read at 1 minute increments for 5 minutes at 412 nm. The amount of GSH or GSSG per total protein was then calculated. We also used a total glutathione kit (Enzo Life Sciences, Plymouth Meeting, PA) as another method to determine total glutathione and GSSG.

***M. abscessus* Growth Assays**

THP-1 cells (5×10^5 /well) were treated with 10 % FBS RPMI media containing phorbol 12-myristate 13-acetate (PMA, 7.5 ng/mL, Sigma, St. Louis, MO) for 24 hours to differentiate the monocytes into a more macrophage-like phenotype. The medium on the adhered cells was replaced with fresh 10% FBS RPMI medium with or without one of several oxidants or antioxidants, including H_2O_2 (5 μ M and 15 μ M, Thermo Fisher Scientific, Waltham, MA), PMA (3.75 ng/mL and 7.5 ng/mL), N-acetyl-L-cysteine (5 mM, 10 mM and 15 mM, Sigma) and MnTE-2-PyP (30 μ M). After 1 hour incubation, the cells were infected with 5×10^6 bacteria/well (for a MOI equal to 10) for 1 hour. For all wells, the infectious medium was removed, the cells were washed with 1:1 mixture of 1X PBS and RPMI, and fresh medium was replaced with or without one of the oxidants or antioxidants. For Day 0 time point, adherent cells were lysed with 0.25% SDS. 7H9 plating broth was then added to neutralize the SDS. Serial dilutions of cell lysates were plated in duplicate on Middlebrook 7H10 agar and bacteria were allowed to grow for 4 days at 37 °C. The numbers of colony-forming units (CFU) on the plates were counted and the mean CFU calculated. Cells at Day 4 and Day 8 after infection were harvested in the same manner as those at the Day 0 time point.

Statistics

All data were derived from at least three independent experiments. The data were analyzed by a one-way ANOVA followed by a Student-Newman-Keuls test or a paired t-test.

Results

Effects of *M. abscessus* infection on SOD mRNA, protein and activity levels

To determine the effect of *M. abscessus* on the intracellular redox state of the infected macrophages, a variety of redox markers were measured. We first investigated the effects of *M. abscessus* infection on superoxide dismutase (SOD) mRNA and protein levels (Figure 1 and 2). Specifically, we measured MnSOD, a mitochondrial superoxide scavenger and Cu/ZnSOD, a cytoplasmic superoxide scavenger in both uninfected and *M. abscessus* infected THP-1 cells. It has been well established that cells under stress produce increased levels of MnSOD [14–16]. *M. abscessus* infection significantly increased MnSOD mRNA levels at 24 and 48 hours post-infection (Figure 1A). Cu/ZnSOD mRNA levels were not significantly affected early on during infection. However, at 48 hours post-infection, Cu/ZnSOD levels were decreased, although this change was not significant (Figure 1B).

MnSOD and Cu/ZnSOD protein levels were then measured by western blot analysis (Figure 2A). In accordance with the mRNA data, MnSOD protein was significantly enhanced with *M. abscessus* infection at 48 and 72 hours post-infection (Figure 2B). Cu/ZnSOD protein was significantly reduced at 72 hours post-infection with *M. abscessus* (Figure 2C). Since densitometry is only semi-quantitative, we also measured MnSOD and Cu/ZnSOD levels by

ELISA (Figure 2D and 2E). We observed the same significant trends; MnSOD is enhanced with infection while Cu/ZnSOD levels are reduced with *M. abscessus* infection. We have previously shown that the antioxidant, MnTE-2-PyP (30 μ M) significantly inhibits *M. abscessus* growth [9]. However, MnTE-2-PyP had no effect on either MnSOD or Cu/ZnSOD protein levels.

We next determined whether or not the SOD proteins produced by the cells were active (Figure 3). A nitroblue tetrazolium in-gel activity assay was performed for MnSOD and Cu/ZnSOD enzymes (Figure 3A). MnSOD activity was enhanced throughout the course of the infection, although MnSOD activity was only significantly increased at 24 hours post-infection (Figure 3B). Cu/ZnSOD activity was decreased at later time points and significantly lower at 72 hours post-infection (Figure 3C). We consistently observed a non-specific band beneath the Cu/ZnSOD band in our samples (Figure 3A). We determined that this band was present in our media and present in FBS as well (Figure 3A). Therefore, we conclude that residual amounts of FBS from the cultured cells are responsible for this non-specific band. We also ran *M. abscessus* bacteria alone on the activity assay to determine if the bacterial SOD could be contributing to the SOD activity observed in the lysed cells. We found no SOD activity from *M. abscessus* in our assay. MnTE-2-PyP also had no significant effect on the activity of either SOD.

***M. abscessus* infection reduces catalase activity in infected THP-1 cells**

Catalase is found in peroxisomes inside cells where it scavenges hydrogen peroxide. An in-gel catalase activity assay was performed on uninfected cells, *M. abscessus* infected cells and *M. abscessus* infected cells in the presence of MnTE-2-PyP (Figure 4A). Catalase activity was already inhibited by *M. abscessus* at 24 hours post-infection and this trend continued through the course of infection (Figure 4B). By 72 hours post-infection, the catalase activity in the infected cells was significantly reduced as compared to uninfected cells (Figure 4B). MnTE-2-PyP had no effect on catalase activity.

Glutathione peroxidase (GPx) activity is inhibited with *M. abscessus* infection

GPx is located in the cytoplasm and functions to convert hydrogen peroxide to water and to prevent lipid peroxidation. GPx activity was measured using a colorimetric assay and was performed on uninfected THP-1 cells, *M. abscessus* infected THP-1 cells and *M. abscessus* infected THP-1 cells in the presence of MnTE-2-PyP (Figure 5). GPx activity declined in infected cells at 24 hours post-infection. By 48 and 72 hours after *M. abscessus* infection, there was significantly reduced GPx activity as compared to uninfected controls (Figure 5). Interestingly, cells infected in the presence of MnTE-2-PyP did not have decreased levels of GPx activities. The levels of GPx activity from cells infected in the presence of MnTE-2-PyP were not significantly different from GPx activity levels obtained from uninfected cells (Figure 5).

***M. abscessus* infection reduces glutathione (GSH) levels inside THP-1 cells**

GSH is also present in the cytoplasm in large quantities and is a major buffering system against ROS in human cells. GSH protects the cell from oxidative stress by scavenging hydrogen peroxides. A reduction in GSH is highly suggestive of an oxidatively stressed cell system. GSH levels were measured via a colorimetric assay in uninfected and *M. abscessus* infected cells (Figure 6). *M. abscessus* infection reduced GSH levels inside THP-1 cells throughout the time course investigated. As shown in Figure 5, GSH levels were significantly reduced in infected cells as compared to non-infected cells at 60 and 240 minutes post-infection. GSSG was not detected in these samples using two different methods (data not shown). Thus, we conclude that total glutathione levels are equivalent to the reduced glutathione.

An oxidizing environment promotes growth of *M. abscessus*

Since *M. abscessus* infections caused an increase in MnSOD levels and a decrease in other antioxidant levels and activities, the results suggest that *M. abscessus* infections produce a more oxidizing environment inside the infected cell. We next determined what effect a more oxidizing environment has on the viability of intracellular *M. abscessus*. Differentiated THP-1 cells were infected with *M. abscessus* in the presence of two oxidizing agents: hydrogen peroxide (0, 5 or 15 μM) or phorbol ester (PMA, 0, 3.75, or 7.5 ng/mL). Hydrogen peroxide is a reactive oxygen species and PMA administration causes superoxide to be produced inside the treated cell [17,18]; therefore, both agents will produce a more oxidizing environment. These are two different species that potentially have different targets within or outside the cell; therefore, the oxidative stress may occur in different areas. An *M. abscessus* growth assay was performed on THP-1 cells lysates in the presence of these two oxidizing reagents (Figure 7). Hydrogen peroxide at 5 and 15 μM significantly promoted *M. abscessus* growth by 8 days post-infection (Figure 7A). PMA promoted *M. abscessus* growth inside THP-1 cells as well; however, this change was not significant (Figure 7B). The viability of the cells was measured in the presence of H_2O_2 to ensure that the cell death was not responsible for the reduction in bacterial growth. The differences in viability of THP-1 cells on day 4 and day 8 cultured with or without H_2O_2 were not significant. On day 4 of culture, cells incubated without H_2O_2 were $88.5\% \pm 3.0\%$ viable, cells incubated with 5 μM H_2O_2 were $88.6\% \pm 2.2\%$ viable and cells incubated with 15 μM H_2O_2 were $83.4\% \pm 2.1\%$ viable. On day 8 of culture, incubated without H_2O_2 were $66.9\% \pm 5.5\%$ viable, cells incubated with 5 μM H_2O_2 were $62.6\% \pm 4.9\%$ viable and cells incubated with 15 μM H_2O_2 were $59.2\% \pm 7.6\%$ viable.

N-acetyl-L-cysteine (NAC) reduces *M. abscessus* growth

We previously showed that MnTE-2-PyP inhibited viability of intracellular *M. abscessus* in THP-1 cells [9]. We wanted to determine if another antioxidant, NAC, could also alter the growth of *M. abscessus*. NAC is a derivative of the amino acid, L-cysteine, and is a precursor in the formation of glutathione. THP-1 cells were infected with *M. abscessus* in the absence or presence of NAC (5, 10, 15 mM) and a *M. abscessus* growth assay was performed on the infected cells (Figure 8). NAC decreased the number of *M. abscessus* isolated in a dose-dependant manner. NAC (10 and 15 mM) significantly inhibited growth of *M. abscessus* at days 4 and 8 post-infection (Figure 8).

Discussion

In the present study, we compared the redox environment of uninfected THP-1 macrophages to *M. abscessus* infected cells. We determined that *M. abscessus* infection caused a significant increase in MnSOD mRNA, protein and activity levels inside the infected macrophages. This finding is not surprising, as several other studies have shown that MnSOD is upregulated within stressed cells to compensate for the more oxidized environment [14–16]. Presumably the increased MnSOD levels would protect the mitochondria from damage and help to promote the survival of the stressed cells.

In contrast, we found that Cu/ZnSOD mRNA, protein and activity levels were decreased with infection. Generally, Cu/ZnSOD levels are unaltered when the cell is in a stressful environment. However, Afonso *et al.* have shown that TNF- α decreases Cu/ZnSOD levels in another monocytic cell line, U937 [19]. We previously showed that *M. abscessus* infections cause an increase in TNF- α levels in THP-1 cells [9]. Thus, in response to infection with *M. abscessus*, enhanced TNF- α release may account for the observed decrease of Cu/ZnSOD mRNA, protein and activity inside the infected cell. Also, at later time points during post-infection, the suppression of Cu/ZnSOD levels may in part be due to increased cell death. In a previous study, we showed that at 2–3 days post-infection the *M. abscessus* infected THP-1

cells had increased levels of apoptosis [9]. To augment this finding we measured cell viability with infection and found that there was a 14% decrease in cell viability 24 hours post-infection, a 30% decrease at 48 hours post-infection and a 58% decrease in cell viability at 72 hours post-infection when compared to uninfected cells. However, we also demonstrated that MnTE-2-PyP protected the infected cell from undergoing cell death [9]. Cu/ZnSOD levels were the same in infected cells treated with MnTE-2-PyP as compared to cells infected alone. Therefore, it is unclear whether cell death may explain the loss of Cu/ZnSOD protein and activity loss.

It is not known if *M. abscessus* has endogenous SOD enzymes. However, it has been well studied that other mycobacteria such as, *M. tuberculosis* and *M. avium*, contain FeSOD, CuSOD and MnSOD enzymes [20,21]. Thus, it is likely that *M. abscessus* also contains SOD enzymes. We did not find any SOD enzyme activity from the bacteria in the SOD in-gel assay. This is probably due to the fact that we ran the samples under native conditions. Mycobacteria have thick, waxy cell walls, which makes it very difficult to lyse open the bacteria. Therefore, we postulate that the native conditions used to assay our samples were not stringent enough to lyse the bacteria to expose the bacterial SOD enzymes. We believe that the SOD activity observed in the in-gel assay is due to the macrophage rather than the bacteria.

We also observed a loss of activity of other antioxidants at later times during the infection. Catalase activity was decreased throughout the infection and was significantly inhibited 72 hours post-infection. Likewise, GPx activity was decreased throughout the course and was significantly inhibited at 48 and 72 hours post-infection. This observation could be caused by high levels of oxidative stress. Catalase activity is inhibited by increased levels of hydrogen peroxide and GPx activity can be lost in the presence of nitric oxide [22,23]. We previously showed that nitric oxide production is enhanced with *M. abscessus* infection [9]. The addition of MnTE-2-PyP had no effect on catalase activity in *M. abscessus* infected cells; however, MnTE-2-PyP did protect from GPx activity loss in *M. abscessus* infected cells. MnTE-2-PyP is known to scavenge hydrogen peroxide. One explanation for the observed difference, is that MnTE-2-PyP may be present in the cytoplasm but not in the peroxisomes. MnTE-2-PyP in the cytoplasm would scavenge hydrogen peroxide and, thus, its activity would be indistinguishable from GPx activity. These data indicates that hydrogen peroxide may play an important role in the growth of *M. abscessus*.

GSH levels were significantly reduced with *M. abscessus* infection at early times during infection. We tried measuring GSSG levels as well, but the low concentration of oxidized glutathione was immeasurable in our assay. Therefore, we can only report on the levels of reduced glutathione. However, the fact that GSH levels were reduced indicates that the cell is likely undergoing oxidative stress.

After reviewing all the results obtained from the intracellular antioxidants measured in this study, we conclude that a cell infected with *M. abscessus* creates an oxidizing environment within the infected cell. MnSOD, an enzyme that is upregulated with stress, is enhanced by *M. abscessus* infection while all the other antioxidants measured were downregulated with *M. abscessus* infection.

We then determined the effect that an oxidizing environment has on the viability of intracellular *M. abscessus*. We created an oxidizing environment by adding H₂O₂ or PMA to THP-1 cells. We found that the addition of H₂O₂ and PMA enhanced *M. abscessus* recovery. We conclude from this finding that the oxidizing environment observed during infection with *M. abscessus* actually promotes the growth of the bacteria within the cell.

We previously reported that MnTE-2-PyP significantly reduced the viability of *M. abscessus* inside THP-1 cells by promoting localization of bacteria to the lysosome [9]. Based on these current findings, it is important to confirm whether another antioxidant could reduce the

number of viable intracellular *M. abscessus*. The potent antioxidant, NAC, was chosen because of its low toxicity and because it is used clinically in man [24]. We found that NAC, in a dose-dependant manner, decreased viability of intracellular *M. abscessus* in THP-1 cells.

In this study we have shown that an oxidizing environment promotes the intracellular growth of *M. abscessus*, while a reducing environment inhibits *M. abscessus* growth. This finding challenges the existing dogma that an oxidizing environment inhibits bacterial growth. While this may be the case for extracellular bacteria like staphylococcus, we believe that an oxidizing environment may be well tolerated by intracellular pathogens and potentially necessary for survival within human cells..

The present study shows that the redox environment within the cell regulates growth of *M. abscessus* and indicates that antioxidants can be used to reduce the intracellular growth of *M. abscessus*. These findings may enhance the current treatment options for patients afflicted with *M. abscessus* infections, which currently only include lengthy antibiotic therapy and surgical resection. This particular mycobacterium is resistant to most antibiotics, making it very difficult to treat. Since MnTE-2-PyP works additively with the antibiotic, clarithromycin, to inhibit *M. abscessus* growth [9], we believe that antioxidant treatment in conjunction with antibiotic therapy may provide better treatment outcomes in patients diagnosed with *M. abscessus* infections. Future studies should also explore the effects a reducing environment has on the viability of other intracellular pathogens.

Acknowledgments

This research was funded by NIH-RO1-HL66112, Potts Foundation Award, the Monfort Foundation, and the Department of Defense. The authors would also like to thank Dr. Christine Weydert for her helpful suggestions.

List of Abbreviations

<i>M. abscessus</i>	<i>Mycobacterium abscessus</i>
<i>M. tuberculosis</i>	<i>Mycobacterium tuberculosis</i>
MnTE-2-PyP	Manganese (II) Meso-Tetrakis-(N-Methylpyridinium-2-yl) porphyrin
NAC	N-acetyl-L-cysteine
NTM	nontuberculous mycobacteria
PMA	phorbol 12-myristate 13-acetate
CFU	colony forming units
SOD	superoxide dismutase
GPx	glutathione peroxidase
GSH	reduced glutathione
BCA	bicinchoninic acid
NBT	nitroblue tetrazolium
ANOVA	analysis of variance
ROS	reactive oxygen species
TNF- α	tumor necrosis factor alpha
MOI	multiplicity of infection

References

1. Petrini B. Mycobacterium abscessus: an emerging rapid-growing potential pathogen. *Apmis* 2006;114:319–328. [PubMed: 16725007]
2. Billinger ME, Olivier KN, Viboud C, de Oca RM, Steiner C, Holland SM, Prevots DR. Nontuberculous mycobacteria-associated lung disease in hospitalized persons, United States, 1998–2005. *Emerging infectious diseases* 2009;15:1562–1569. [PubMed: 19861046]
3. Cassidy PM, Hedberg K, Saulson A, McNelly E, Winthrop KL. Nontuberculous mycobacterial disease prevalence and risk factors: a changing epidemiology. *Clin Infect Dis* 2009;49:e124–e129. [PubMed: 19911942]
4. Lai CC, Tan CK, Chou CH, Hsu HL, Liao CH, Huang YT, Yang PC, Luh KT, Hsueh PR. Increasing incidence of nontuberculous mycobacteria, Taiwan, 2000–2008. *Emerging infectious diseases* 2010;16:294–296. [PubMed: 20113563]
5. Marras TK, Chedore P, Ying AM, Jamieson F. Isolation prevalence of pulmonary non-tuberculous mycobacteria in Ontario, 1997–2003. *Thorax* 2007;62:661–666. [PubMed: 17311842]
6. Colombo RE, Hill SC, Claypool RJ, Holland SM, Olivier KN. Familial clustering of pulmonary nontuberculous mycobacterial disease. *Chest* 2010;137:629–634. [PubMed: 19858235]
7. van Ingen J, de Zwaan R, Dekhuijzen RP, Boeree MJ, van Soolingen D. Clinical relevance of *Mycobacterium chelonae*-abscessus group isolation in 95 patients. *The Journal of infection* 2009;59:324–331. [PubMed: 19732795]
8. Ballarino GJ, Olivier KN, Claypool RJ, Holland SM, Prevots DR. Pulmonary nontuberculous mycobacterial infections: antibiotic treatment and associated costs. *Respiratory medicine* 2009;103:1448–1455. [PubMed: 19467851]
9. Oberley-Deegan RE, Lee YM, Morey GE, Cook DM, Chan ED, Crapo JD. The antioxidant mimetic, MnTE-2-PyP, reduces intracellular growth of *Mycobacterium abscessus*. *American journal of respiratory cell and molecular biology*. 2008
10. Meylan PR, Richman DD, Kornbluth RS. Reduced intracellular growth of mycobacteria in human macrophages cultivated at physiologic oxygen pressure. *The American review of respiratory disease* 1992;145:947–953. [PubMed: 1554224]
11. Mita M, Satoh M, Shimada A, Okajima M, Azuma S, Suzuki JS, Sakabe K, Hara S, Himeno S. Metallothionein is a crucial protective factor against *Helicobacter pylori*-induced gastric erosive lesions in a mouse model. *American journal of physiology* 2008;294:G877–G884. [PubMed: 18239062]
12. Snelgrove RJ, Edwards L, Rae AJ, Hussell T. An absence of reactive oxygen species improves the resolution of lung influenza infection. *European journal of immunology* 2006;36:1364–1373. [PubMed: 16703568]
13. Weydert CJ, Cullen JJ. Measurement of superoxide dismutase, catalase and glutathione peroxidase in cultured cells and tissue. *Nature protocols* 2010;5:51–66.
14. Macmillan-Crow LA, Cruthirds DL. Invited review: manganese superoxide dismutase in disease. *Free radical research* 2001;34:325–336. [PubMed: 11328670]
15. Miao L, St Clair DK. Regulation of superoxide dismutase genes: implications in disease. *Free radical biology & medicine* 2009;47:344–356. [PubMed: 19477268]
16. Pardo M, Tirosh O. Protective signalling effect of manganese superoxide dismutase in hypoxia-reoxygenation of hepatocytes. *Free radical research* 2009;43:1225–1239. [PubMed: 19905985]
17. Datta R, Yoshinaga K, Kaneki M, Pandey P, Kufe D. Phorbol ester-induced generation of reactive oxygen species is protein kinase c β -dependent and required for SAPK activation. *The Journal of biological chemistry* 2000;275:41000–41003. [PubMed: 11042219]
18. Traore K, Sharma R, Thimmulappa RK, Watson WH, Biswal S, Trush MA. Redox-regulation of Erk1/2-directed phosphatase by reactive oxygen species: role in signaling TPA-induced growth arrest in ML-1 cells. *Journal of cellular physiology* 2008;216:276–285. [PubMed: 18270969]
19. Afonso V, Santos G, Collin P, Khatib AM, Mitrovic DR, Lomri N, Leitman DC, Lomri A. Tumor necrosis factor- α down-regulates human Cu/Zn superoxide dismutase 1 promoter via JNK/AP-1 signaling pathway. *Free radical biology & medicine* 2006;41:709–721. [PubMed: 16895791]

20. Malik ZA, Iyer SS, Kusner DJ. Mycobacterium tuberculosis phagosomes exhibit altered calmodulin-dependent signal transduction: contribution to inhibition of phagosome-lysosome fusion and intracellular survival in human macrophages. *J Immunol* 2001;166:3392–3401. [PubMed: 11207296]
21. Spagnolo L, Toro I, D’Orazio M, O’Neill P, Pedersen JZ, Carugo O, Rotilio G, Battistoni A, Djinovic-Carugo K. Unique features of the sodC-encoded superoxide dismutase from Mycobacterium tuberculosis, a fully functional coppercontaining enzyme lacking zinc in the active site. *The Journal of biological chemistry* 2004;279:33447–33455. [PubMed: 15155722]
22. Chaudiere J, Ferrari-Iliou R. Intracellular antioxidants: from chemical to biochemical mechanisms. *Food Chem Toxicol* 1999;37:949–962. [PubMed: 10541450]
23. Miyamoto Y, Koh YH, Park YS, Fujiwara N, Sakiyama H, Misonou Y, Ookawara T, Suzuki K, Honke K, Taniguchi N. Oxidative stress caused by inactivation of glutathione peroxidase and adaptive responses. *Biological chemistry* 2003;384:567–574. [PubMed: 12751786]
24. Gupta AK, Chan GM, Greller HA, Su MK. NAC: still the way to go. *Critical care (London, England)* 2009;13:411. author reply 411.

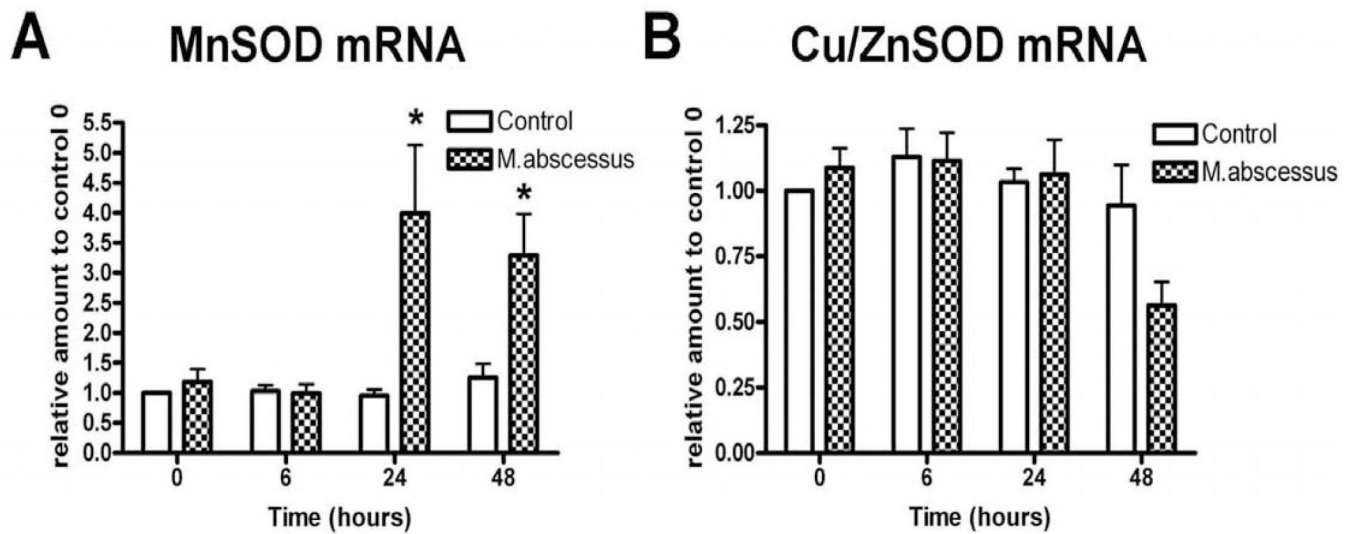


Figure 1. SOD mRNA levels are altered with *M. abscessus* infection

Differentiated THP-1 cells were uninfected (control), infected with *M. abscessus* for the indicated times. Cells were harvested at the times indicated and mRNA was isolated. A. Real Time RT-PCR analysis for MnSOD mRNA levels. MnSOD mRNA was significantly elevated with infection. B. Real Time RT-PCR analysis for Cu/ZnSOD mRNA levels. Cu/ZnSOD mRNA levels were unchanged early during infection; however, at 48 hours post-infection Cu/ZnSOD levels declined (not significant). All data represent the mean \pm SEM, n=4. The asterisk (*) denotes significant change from the respective control ($p < 0.05$).

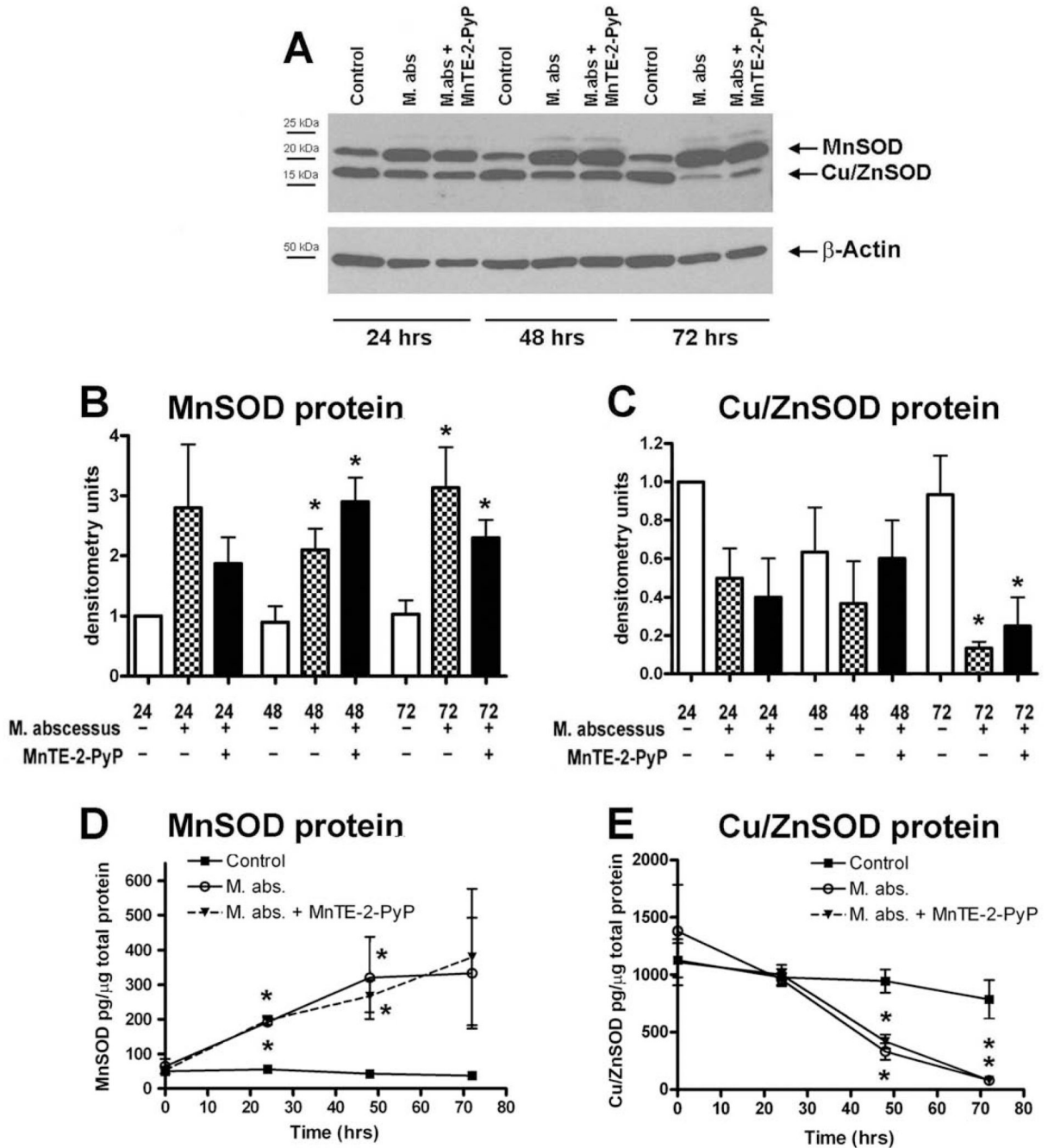


Figure 2. SOD protein levels are altered with *M. abscessus* infection

Differentiated THP-1 cells were uninfected (control), infected with *M. abscessus* or infected in the presence of MnTE-2-PyP for the indicated times. Cells were harvested at the times indicated and protein was isolated. A. A representative western blot for MnSOD and Cu/ZnSOD proteins. B&C. Densitometric analysis of MnSOD and Cu/ZnSOD blots. B. MnSOD protein levels are significantly enhanced at 48 and 72 hours post-infection as compared to uninfected cells for their respective time points. C. Cu/ZnSOD protein levels were significantly reduced 72 hours post-infection. D. MnSOD protein measured by ELISA. E. Cu/ZnSOD protein levels measured by ELISA. The ELISA data was normalized to total protein levels in each sample. All western blot data were normalized to the 24 hour uninfected time point for

the respective SOD protein. For a protein loading control, blots were incubated with a β -actin antibody. Western blot data represent the mean \pm SEM, n=4 and ELISA data represent the mean \pm SEM, n=3. The asterisk (*) denotes significant change from the respective control ($p < 0.05$).

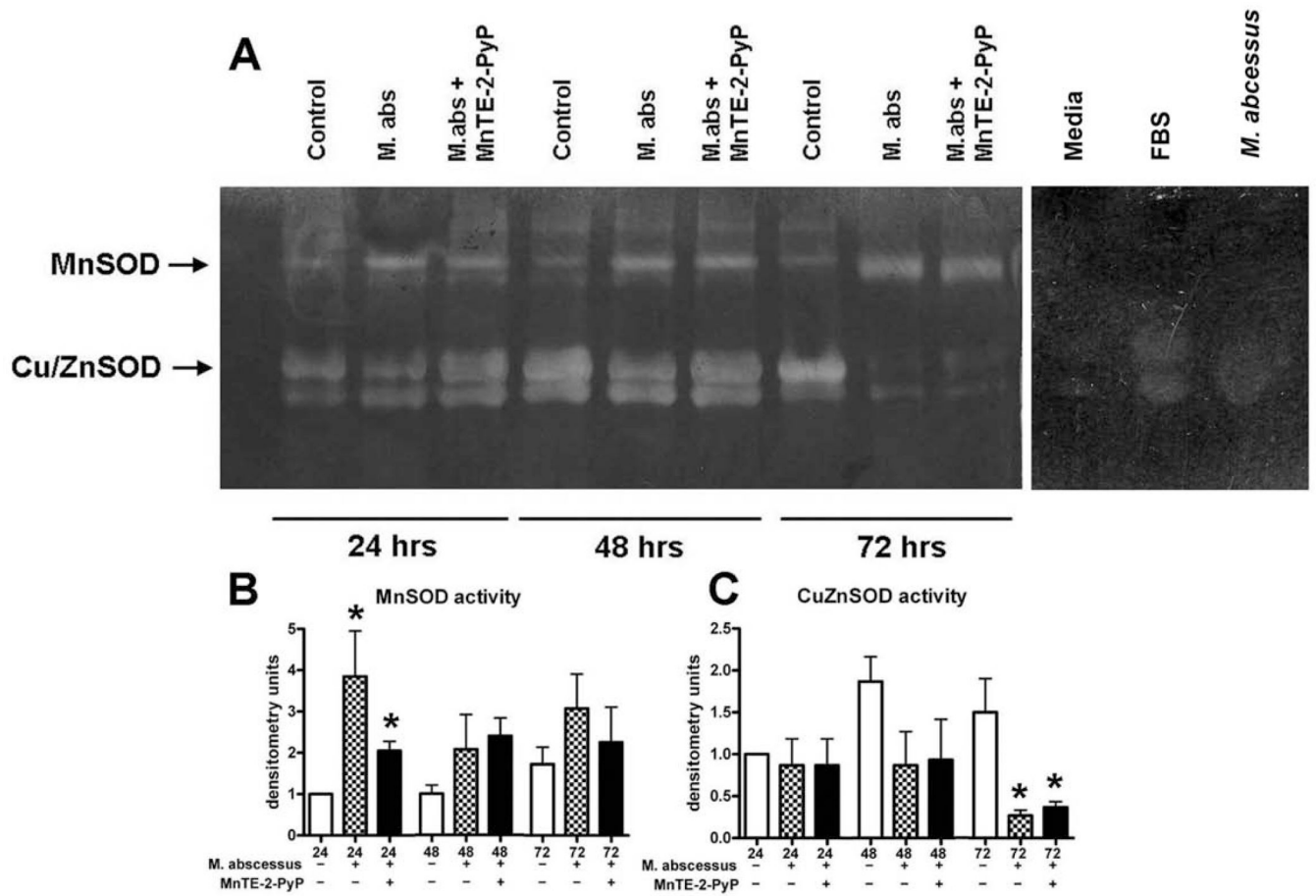


Figure 3. SOD activity is altered with *M. abscessus* infection

Differentiated THP-1 cells were uninfected (control), infected with *M. abscessus* (*M. abs*) or infected in the presence of MnTE-2-PyP (*M. abs* + MnTE-2-PyP) for 24, 48 or 72 hours. A. A representative nitroblue tetrazolium gel. B. Densitometric analysis of MnSOD activity. MnSOD activity was significantly enhanced in infected cells as compared to uninfected cells at 24 hours post-infection. At 48 and 72 hours post-infection MnSOD activity was enhanced in infected cells as compared to control (not significant). C. Densitometric analysis of Cu/ZnSOD activity. Cu/ZnSOD activity was significantly decreased at 72 hours post-infection in *M. abscessus* infected cells as compared to uninfected cells. All data was made relative to the 24 hour uninfected time point for the respective SOD. For controls, media, FBS and *M. abscessus* were analyzed for SOD activity. All data represent the mean \pm SEM, n=4. The asterisk (*) denotes significant change from the respective control ($p < 0.05$).

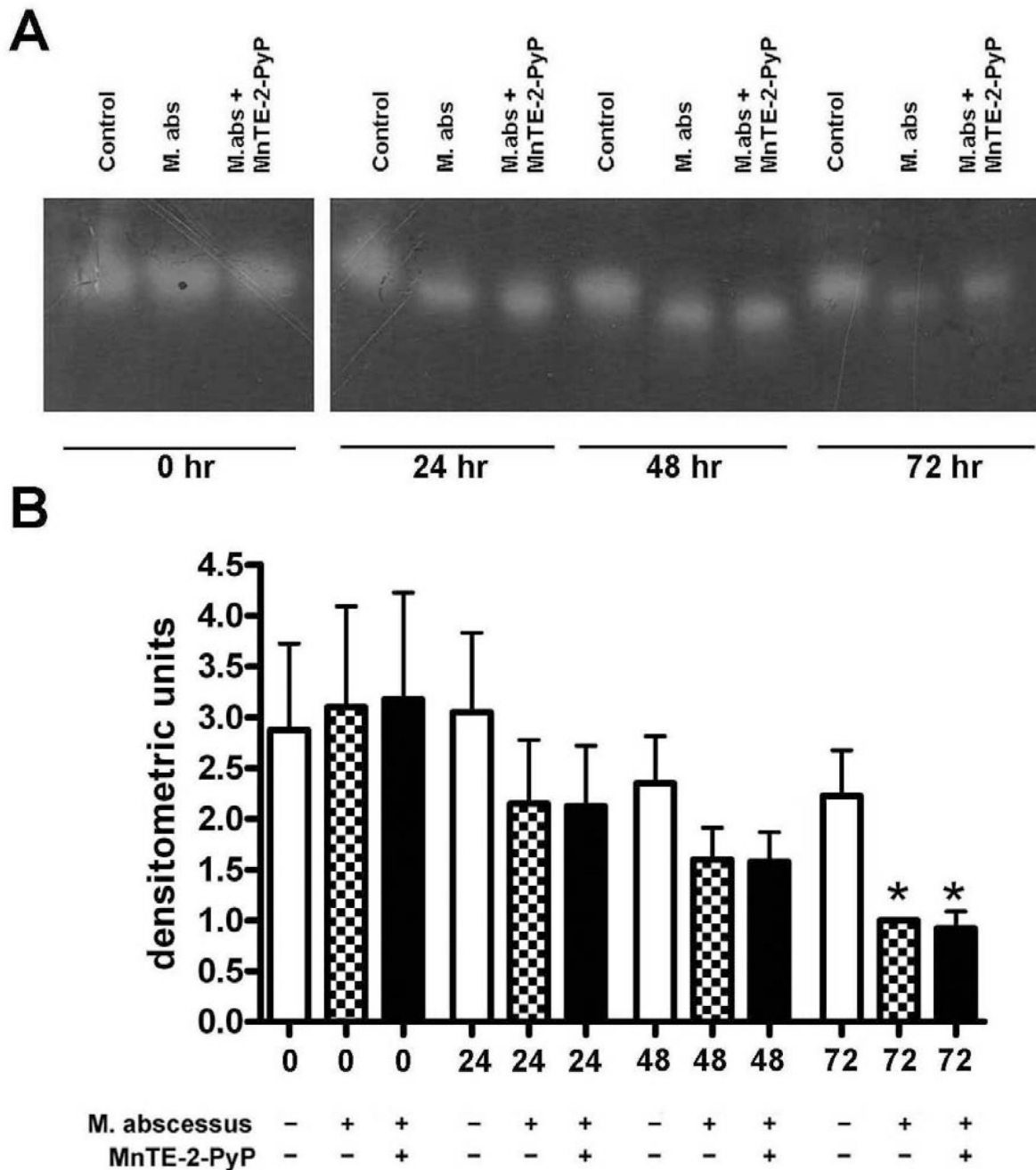


Figure 4. Catalase activity is decreased with *M. abscessus* infection

Differentiated THP-1 cells were uninfected (control), infected with *M. abscessus* (*M. abs*) or infected in the presence of MnTE-2-PyP (*M. abs* + MnTE-2-PyP) for 0, 24, 48 or 72 hours. A. A representative catalase activity gel. B. Densitometric analysis of catalase activity. Catalase activity was significantly reduced in infected cells as compared to non-infected cells at 72 hours post-infection. Catalase activity was decreased with infection at 24 and 48 hours post-infection (not significant). MnTE-2-PyP did not affect catalase activity. All data represent the mean \pm SEM, n=4. The asterisk (*) denotes significant change from the respective control ($p < 0.05$).

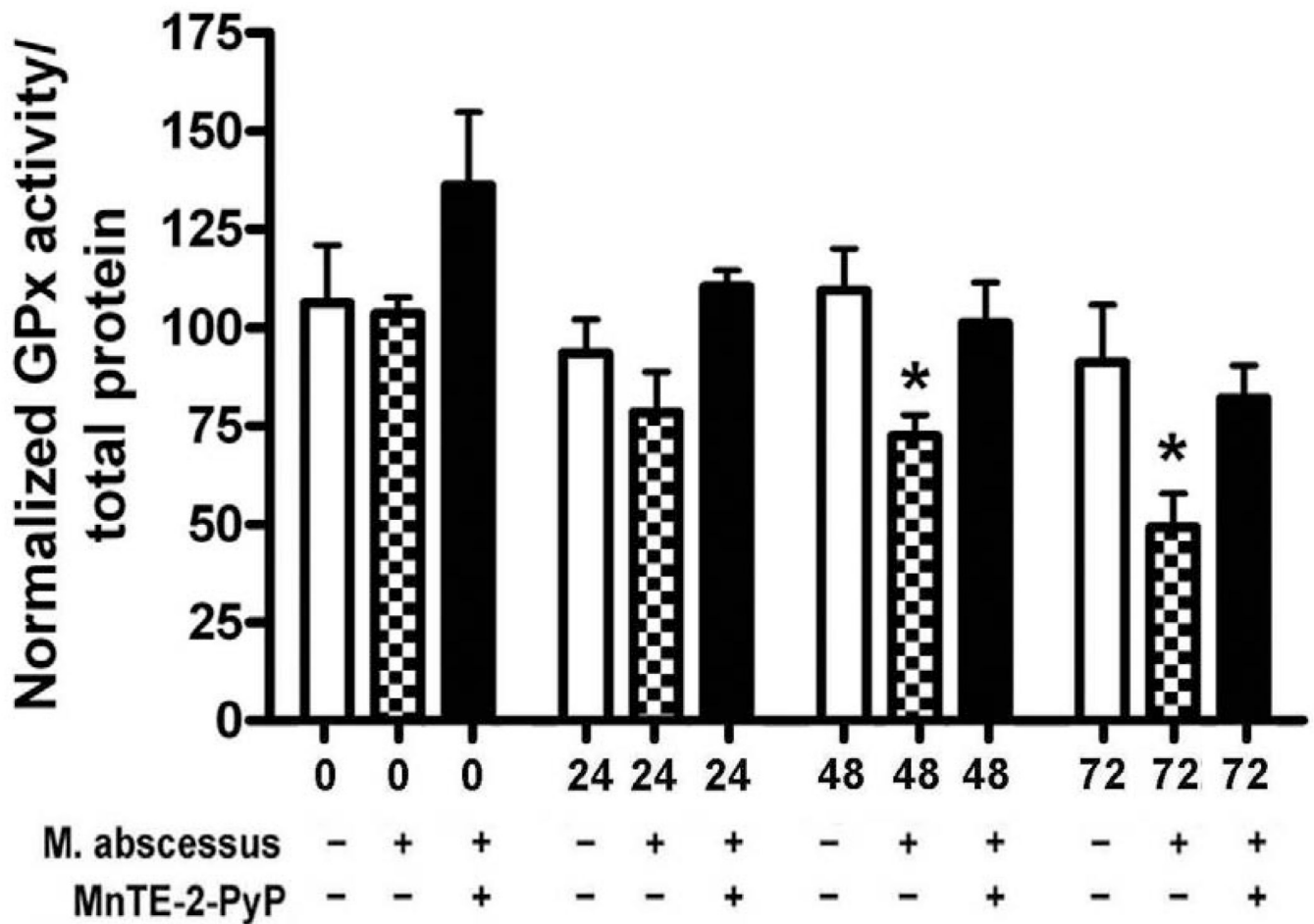


Figure 5. Glutathione peroxidase (GPx) activity is decreased with *M. abscessus* infection
 Differentiated THP-1 cells were uninfected, infected with *M. abscessus* or infected in the presence of MnTE-2-PyP for 0, 24, 48 or 72 hours. GPx activity was significantly decreased in cells infected with *M. abscessus* alone when compared to uninfected cells or cells infected in the presence of MnTE-2-PyP at 48 and 72 hours post-infection. Each experiment was normalized to the control 0 time point. All data represent the mean \pm SEM, n=5. The asterisk (*) denotes significant change from the respective control ($p < 0.05$).

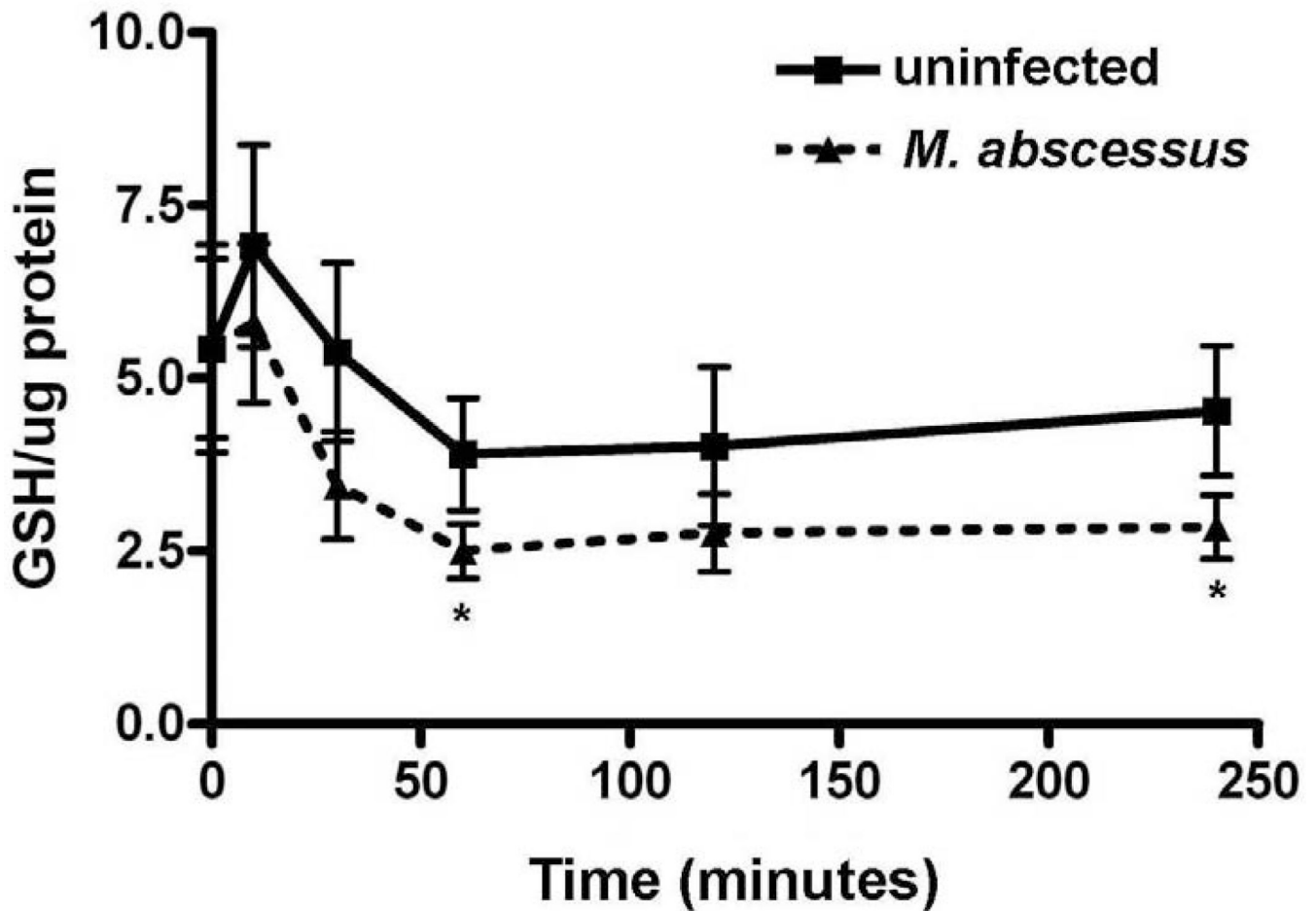


Figure 6. Glutathione (GSH) levels are decreased with *M. abscessus* infection
Differentiated THP-1 cells were uninfected or infected with *M. abscessus* for 0, 5, 30, 60, 120 or 240 minutes post-infection. GSH was measured using a colorimetric assay and was decreased by infection with *M. abscessus*. All data represent the mean \pm SEM, n=5. The asterisk (*) denotes significant change from the respective control ($p < 0.05$).

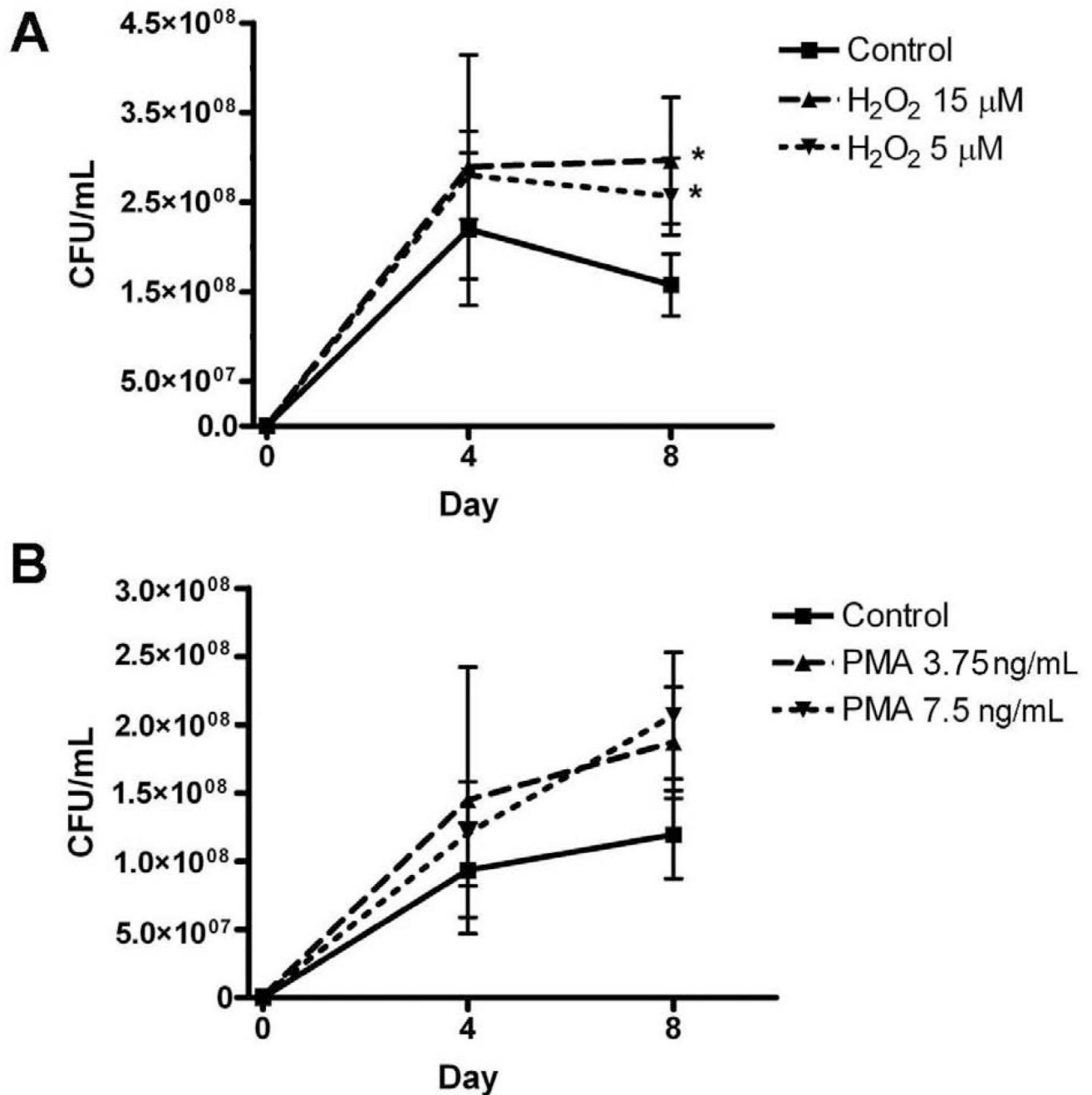


Figure 7. An oxidative environment promotes the intracellular viability of *M. abscessus*
 A. Hydrogen peroxide (H₂O₂) significantly enhanced *M. abscessus* growth at day 8 post-infection. B. PMA enhanced growth of *M. abscessus* at days 4 and 8 post-infection; however this increase was not statistically significant. All data represent the mean ± SEM, n=3. The asterisk (*) denotes significant change from the respective control (p< 0.05).

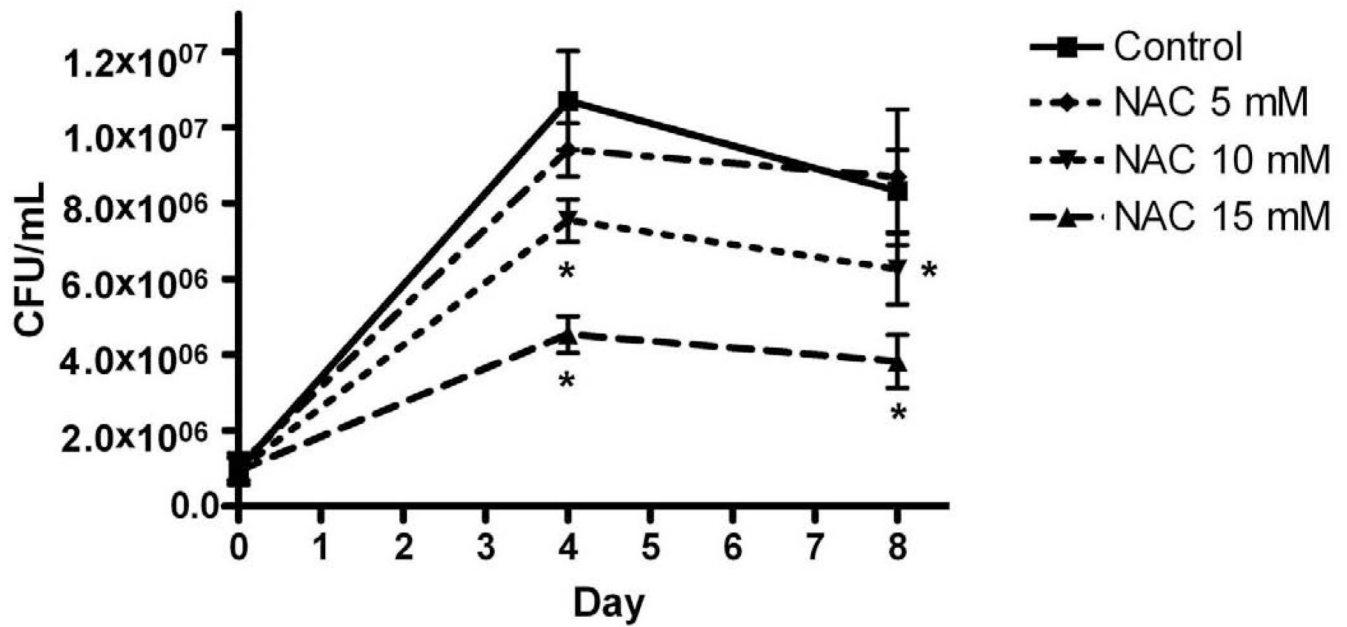


Figure 8. N-acetyl-L-cysteine (NAC) inhibits intracellular growth of *M. abscessus*

Differentiated THP-1 cells were pre-incubated for one hour in RPMI medium or medium containing NAC (5, 10, 15 mM) and infected with *M. abscessus* for one hour (MOI=10). Cells were harvested one hour post-infection (d0), 4 and 8 days post-infection. Cells incubated with NAC (10 and 15 mM) had significantly reduced bacterial numbers on days 4 and 8 post-infection. All data represent the mean \pm SEM, n=5. The asterisk (*) denotes significant change from the infected alone condition (control, $p < 0.05$).